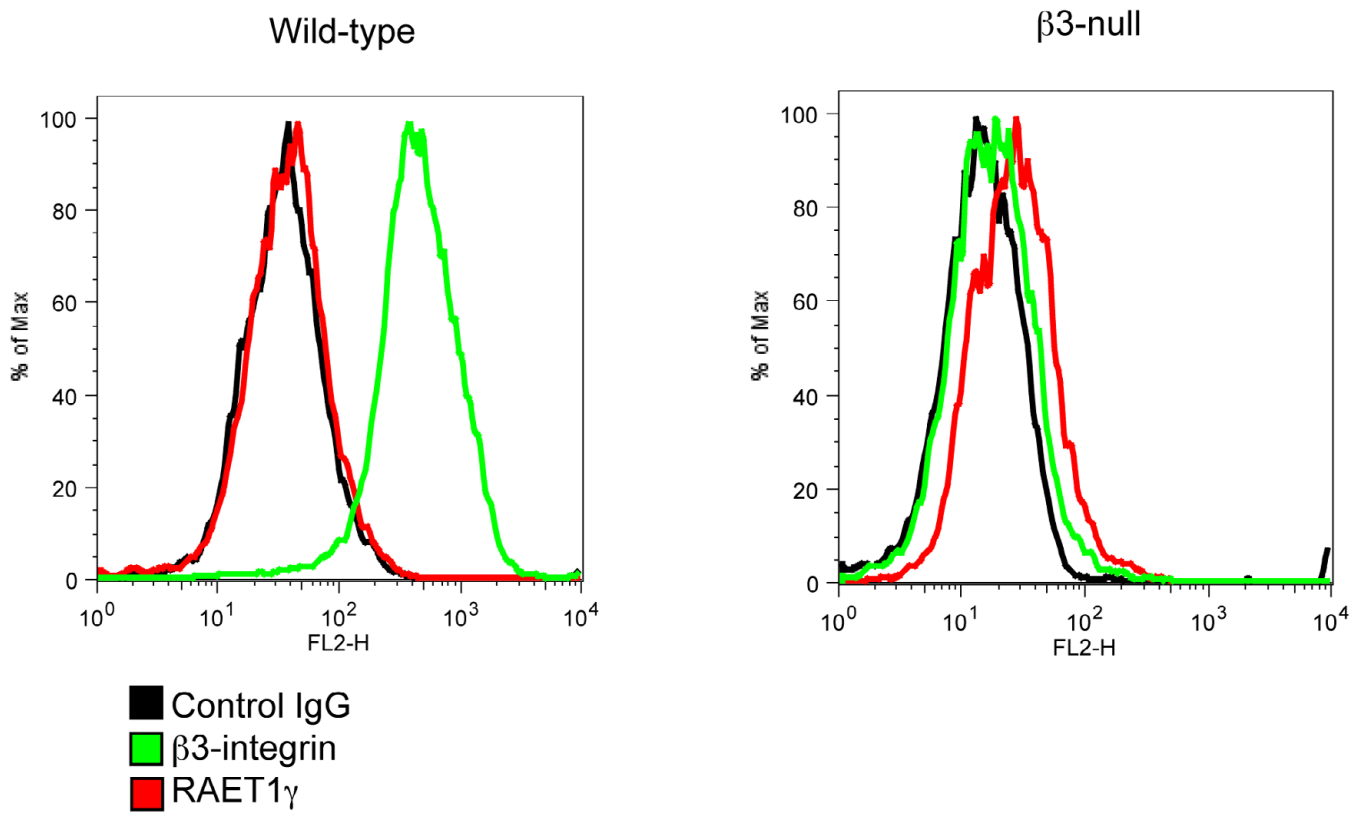

Fig. S1. Flow cytometric analysis of RAET1γ surface expression in wild-type and β3-null endothelial cells. RAET1γ was not detectable on the surface of mouse endothelial cells. Mouse IgG1 was used as negative control, and antibody against β3-integrin was used to confirm β3-integrin deficiency in β*3*-null endothelial cells.

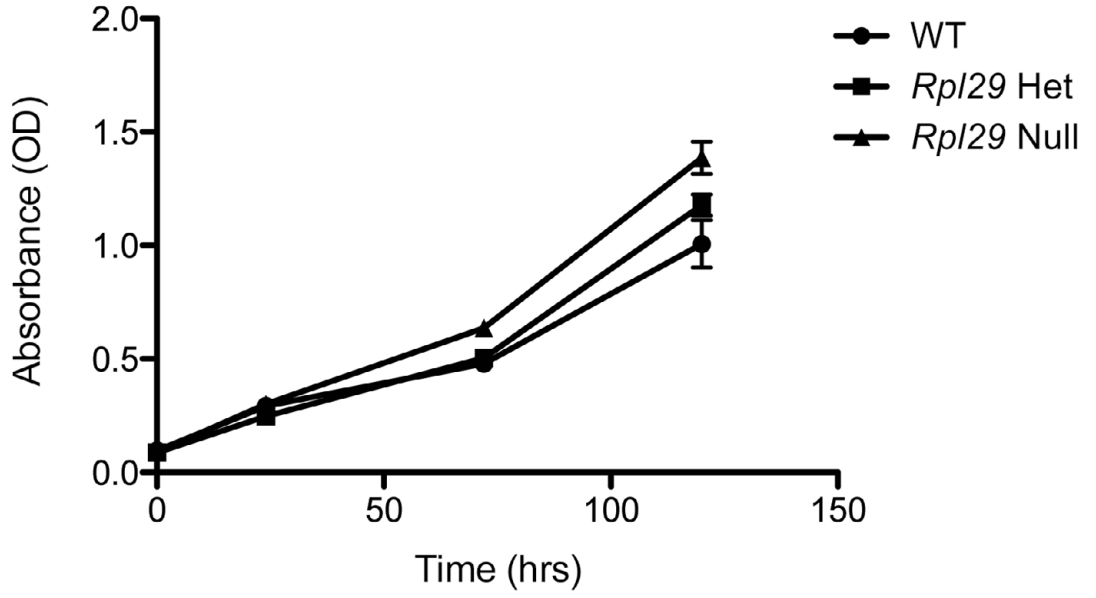

Fig. S2. Cell proliferation assay of wild-type, Rpl29-heterozygous and Rpl29-null endothelial cells. Two thousand cells were seeded into each well of a 96-well plate (Coultar) pre-coated with a mixture of PureCol (Nutacon, Netherlands), human plasma fibronectin (Millipore) and 0.1% gelatine. Cell viability was measured using cell proliferation reagent WST1 (Roche) following manufacturer's protocol at different time points. No reduction in viability was observed in *Rpl29*-heterozygous and *Rpl29*-null endothelial cells in comparison to wild-type endothelial cells (n=3, mean ± s.e.m.).

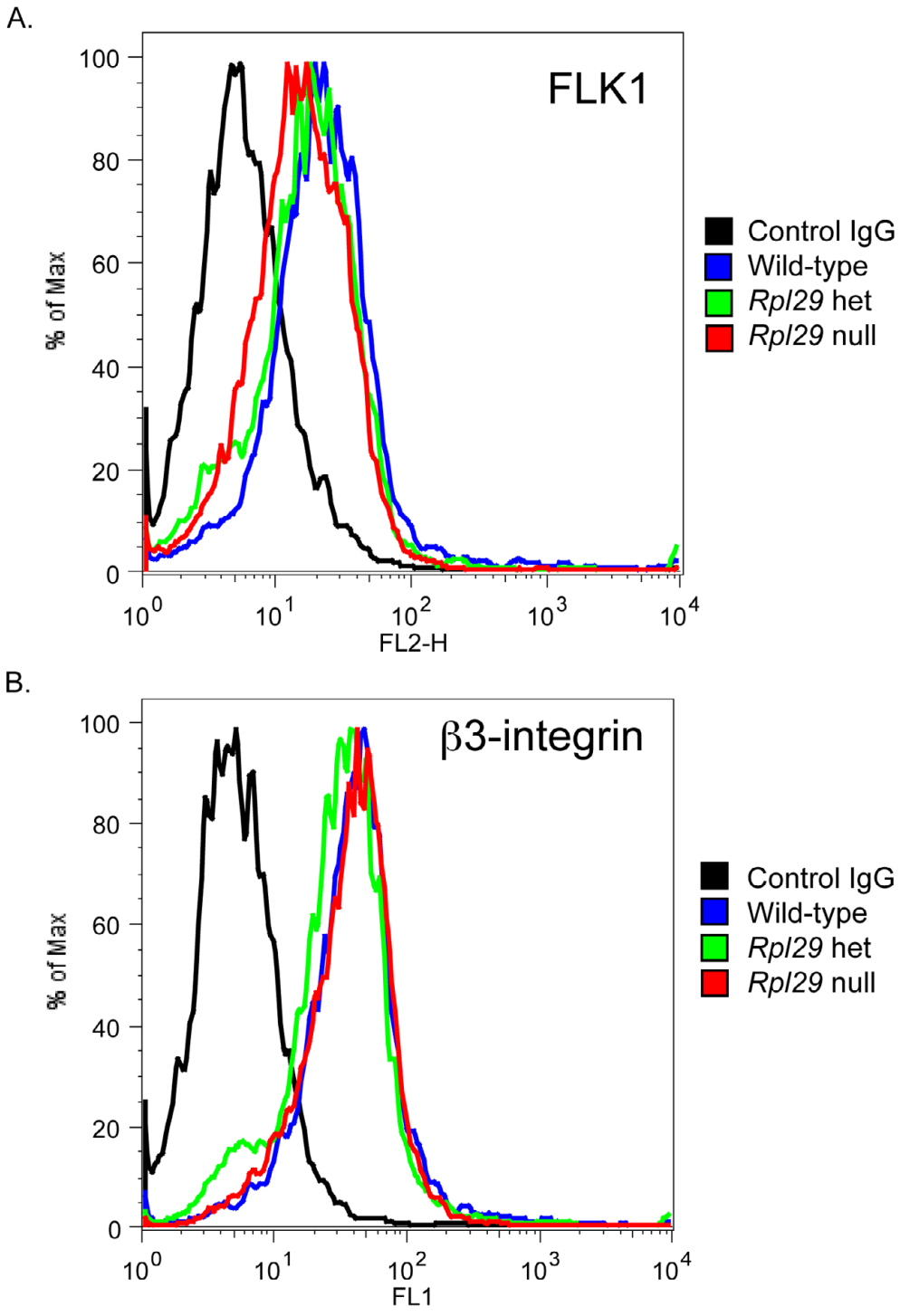

Fig. S3. Flow cytometric analysis of FLK1 and β3-integrin in Rpl29-wild-type, Rpl29-heterozygous and Rpl29-null primary endothelial cells. Mouse IgG1 was used as negative control. No changes in surface expression of either (A) FLK1 or (B) β3 integrin were observed in *Rpl29*-heterozygous or *Rpl29*-null endothelial cells when compared with wild-type controls.

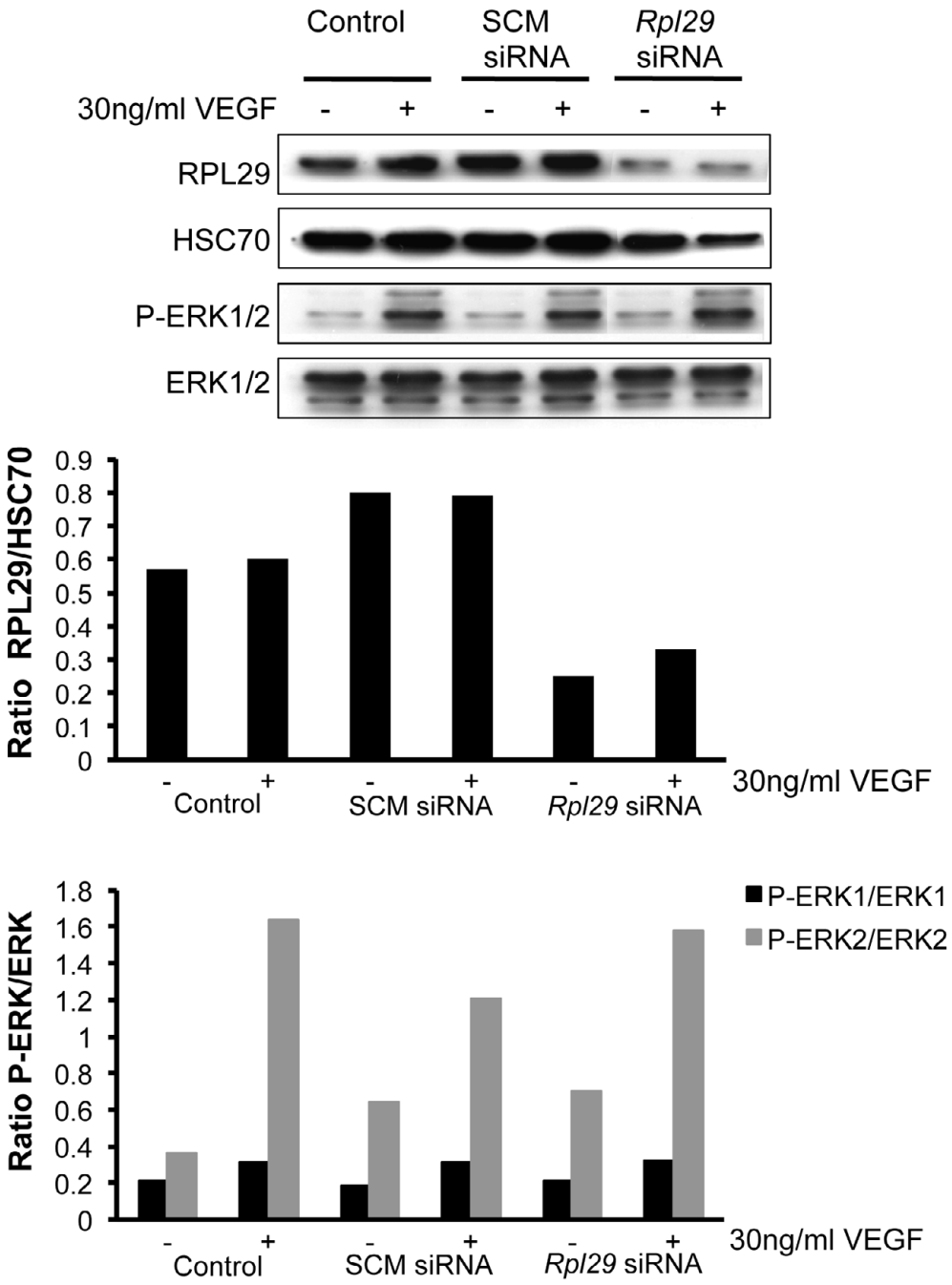

Fig. S4. VEGF-stimulated ERK-phosphorylation. Western blot analysis of pERK1/2 levels to total ERK1/2 in endothelial cells treated with SCM and *Rpl29*-siRNA show that pERK1/2 protein levels were not decreased following *Rpl29* knockdown with siRNA in comparison to SCM-siRNA when cells were exposed to VEGF. Bar charts represent densitometry readings of RPL29 levels were compared to loading control HSC70 and pERK1/2 protein levels relative to total ERK1/2.

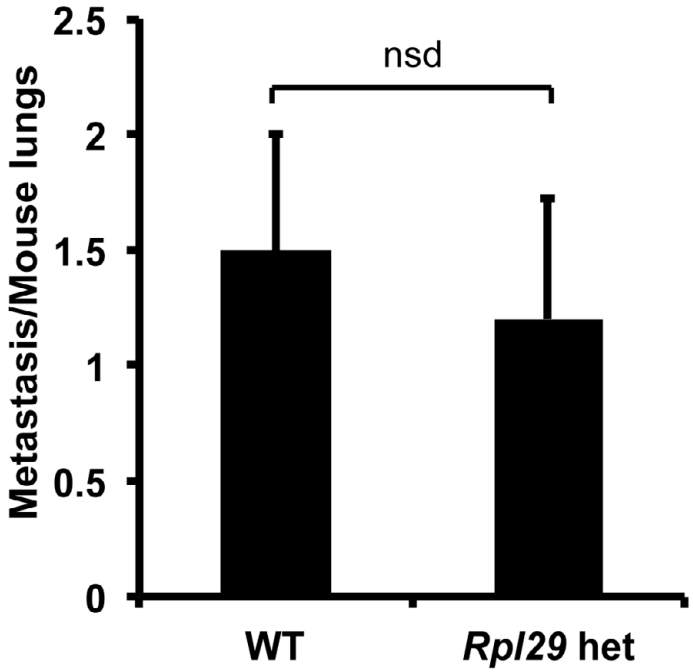

Fig. S5. Metastatic analysis of LLC grown in wild-type and Rpl29-heterozygous mice. Lewis Lung Carcinoma tumour cells (0.5 x 10^6 cells) were injected subcutaneously into the flank of 8-week-old WT and *Rpl29*-heterozygous mice and tumours were allowed to grow for 14 days. Size-matched tumours were ressected and tumours allowed to metastasise to the lungs. The mice were then killed 6 weeks later at which point they showed no adverse effects. Lungs were removed from the mice and examined for surface metastases. No significant difference in lung metastasis was observed between wild-type and Rpl29-null mice. Metastasis was measured by counting LLC metastasis on the surface of lungs/mouse (*n*=4-5, mean ± s.e.m.).

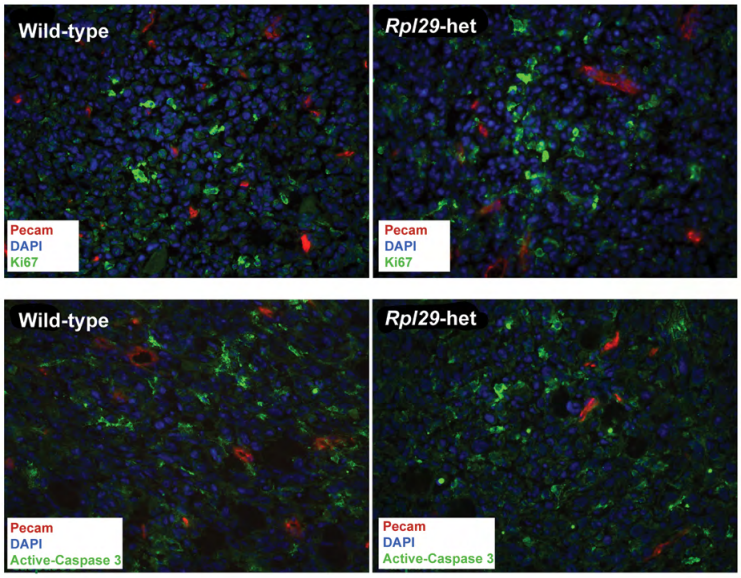

Fig. S6. Tumour proliferation and apoptosis analysis. No gross difference was observed in cell proliferation and apoptosis in LLC tumours from wild-type and *Rpl29*-heterozygous mice. Representative images of Ki67, Active-Caspase-3 and PECAM staining in size matched age matched LLC tumours grown in wild-type and *Rpl29*-heterozygous mice. Sections were counter stained with DAPI to reveal nuclei.

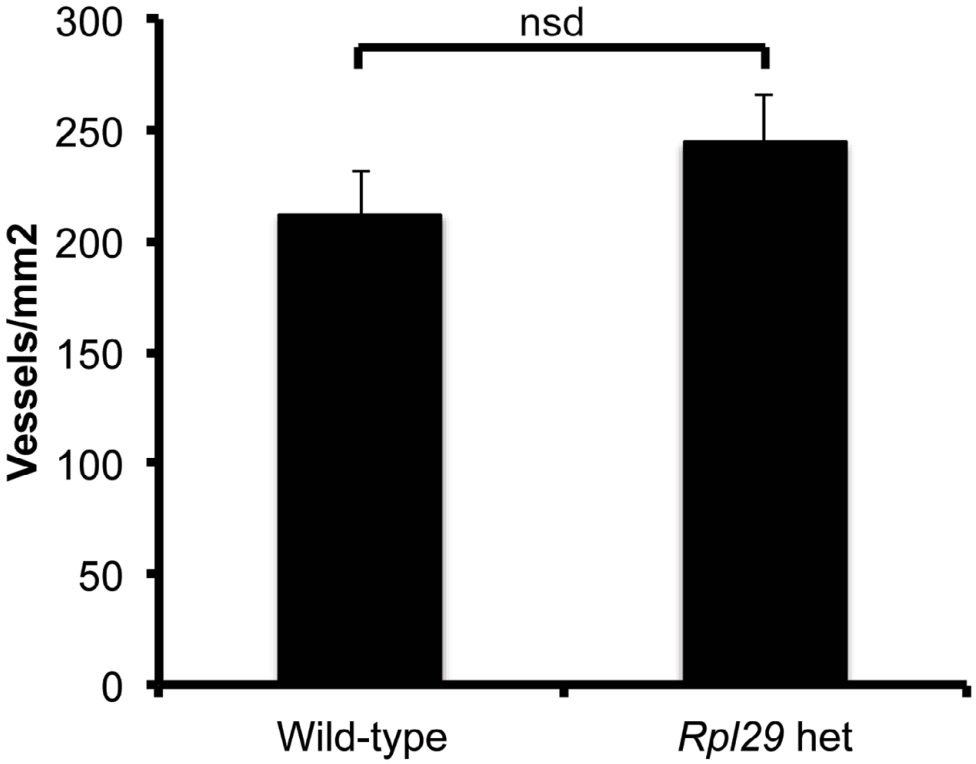

Fig. S7. Blood vessels density in the skin from wild-type and Rpl29-heterozygous mice. No significant difference was observed in blood vessel density in the skin between wild-type and *Rpl29*-heterozygous mice. Bar chart represents mean number blood vessels/mm^2 of dermal section (mean ± s.e.m.; n=7 mice per genotype; nsd, not significant).

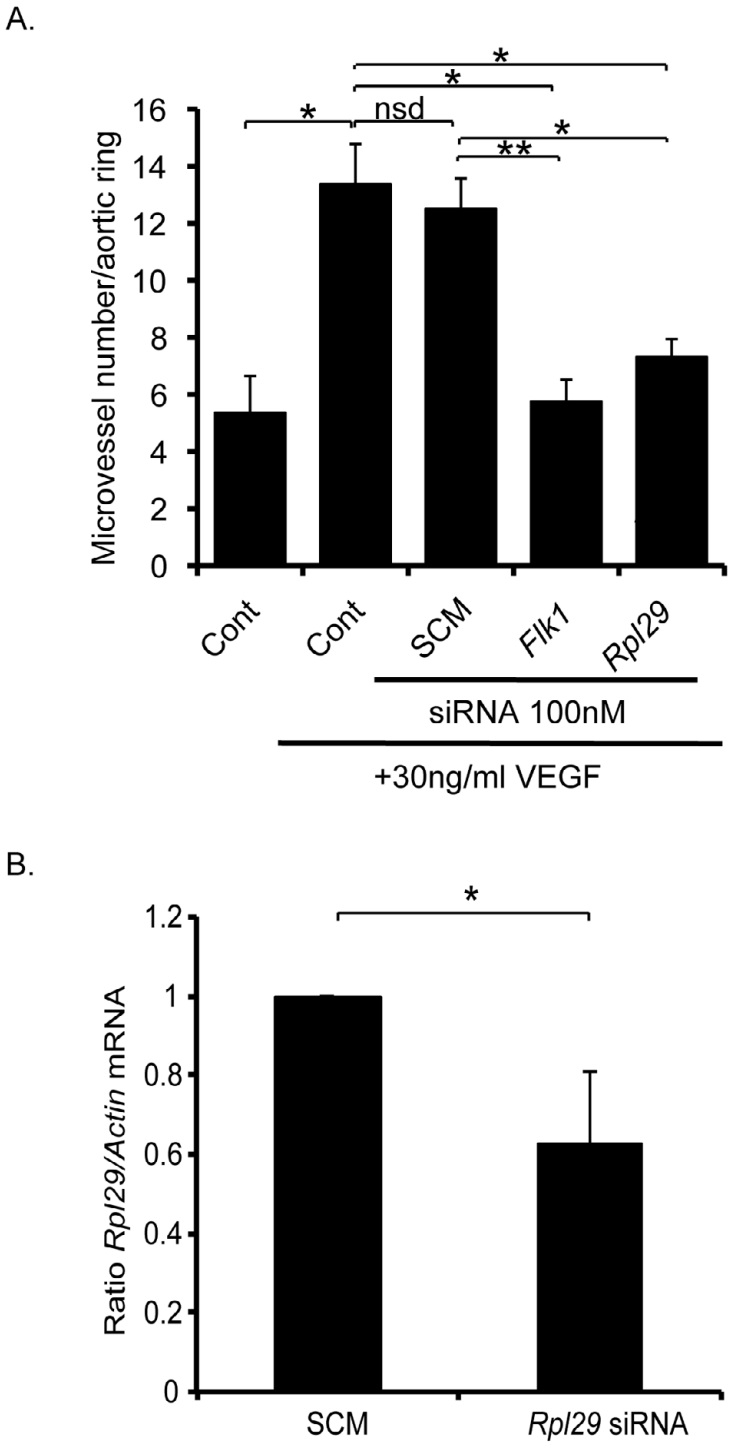

Fig. S8. Aortic ring assay following Rpl29-siRNA treatment. Depletion of Rpl29 with siRNA inhibits microvessel sprouting in β3-null aortic rings. (A) Quantitation of VEGF stimulated microvessel sprouting following treatment with SCM, *Rpl29* or *Flk1* siRNA in β*3*-null aortic rings on day 8. VEGF stimulated the number of microvessel sprouts emerging for aortic rings in Cont and SCM-siRNA treated samples. *Rpl29*-depletion reduced VEGF-stimulated microvessel sprouting to level similar to *Flk1*-depletion (mean ± s.e.m., **P*<0.05, ***P*<0.01, *n*=12-20 aortic rings per treatment). (B) Real-time PCR to validate knockdown of *Rpl29* in aortic rings following treatment with either 100nM SCM or *Rpl29* siRNA (mean ± s.e.m.,***P* <0.01, *n*=3 per group).

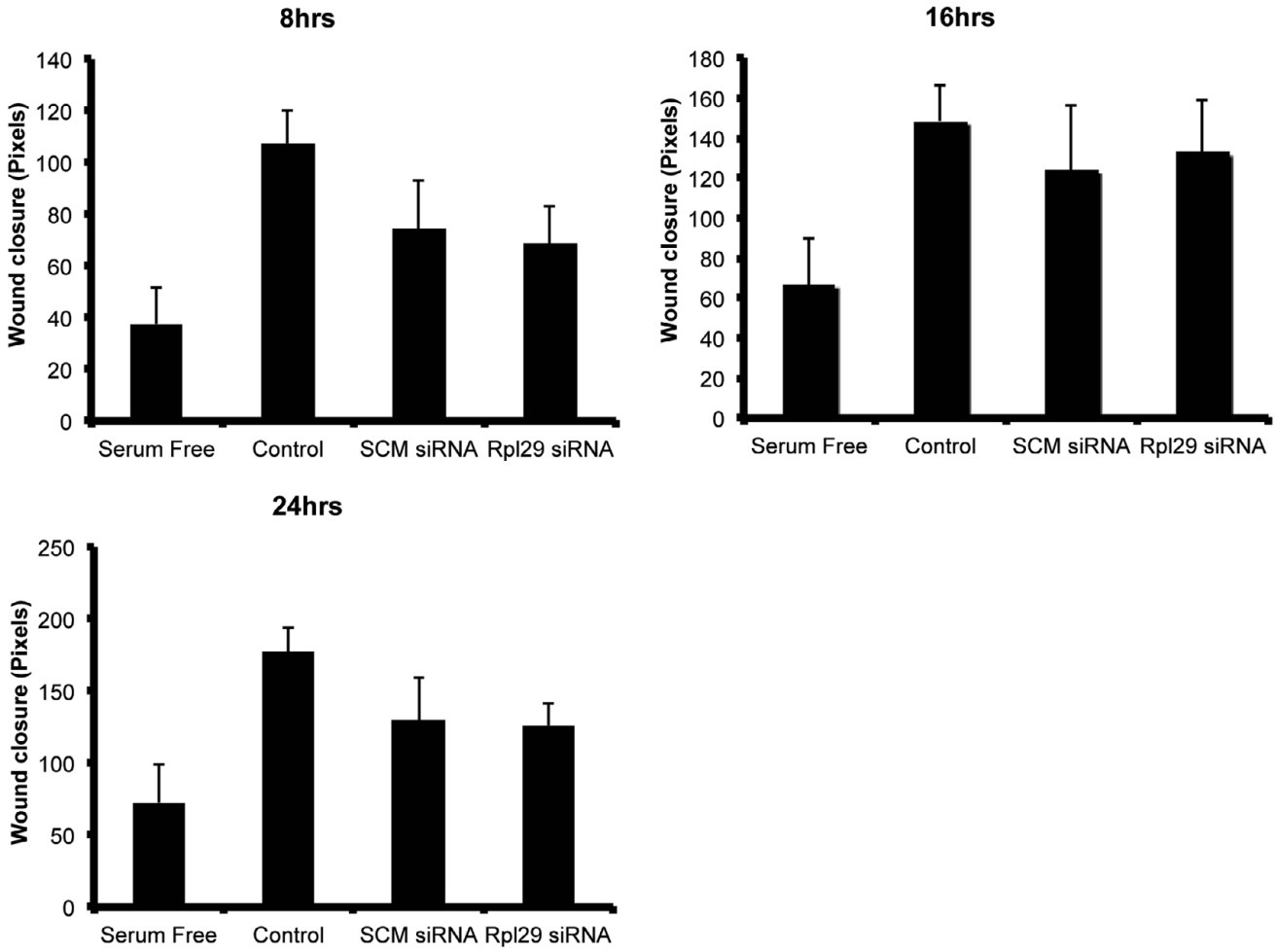

Fig. S9. Cell proliferation assay of PMT-endothelial cells treated with Rpl29 siRNA. No significant difference was observed in endothelial cell proliferation following *Rpl29* siRNA treatment in comparison to SCM siRNA and control sample using WST-1 assay (n=3, mean ± s.e.m.).

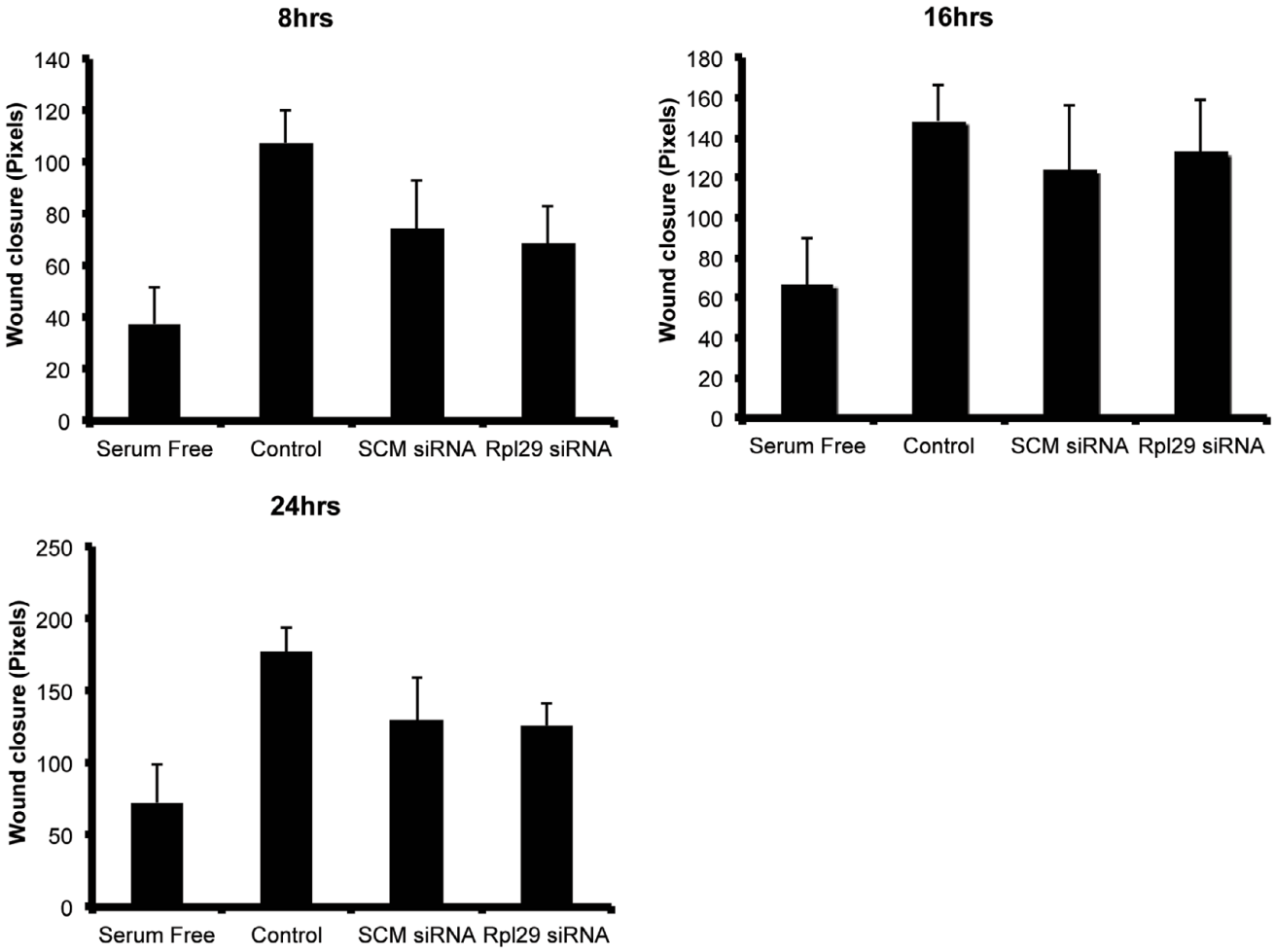

Fig. S10. Cell migration assay. Six-well plates were coated with a mixture of PureCol (Nutacon), human plasma fibronectin (Millipore), and 0.1% gelatine and seeded with 300,000 endotheilal cells per well. Cells were allowed to proliferate until confluent, washed with Opti-MEM and incubated for 2 hours in Opti-MEM 2.5% FCS. Cells in each well were scratched in a straight line with a P200 tip, and media was exchanged with a fresh Opti-MEM 2.5% FCS media with or without 30 ng/ml VEGFA. An inverted time-lapse microscope was used to follow wound healing due to cell migration for up to 24 hours, and data was analysed using ImageJ. No significant difference was observed in serum-stimulated endothelial cell migration between 8 and 24 hours between samples treated with *Rpl29* and SCM siRNA. Values are given as representations of wound closure in pixels.

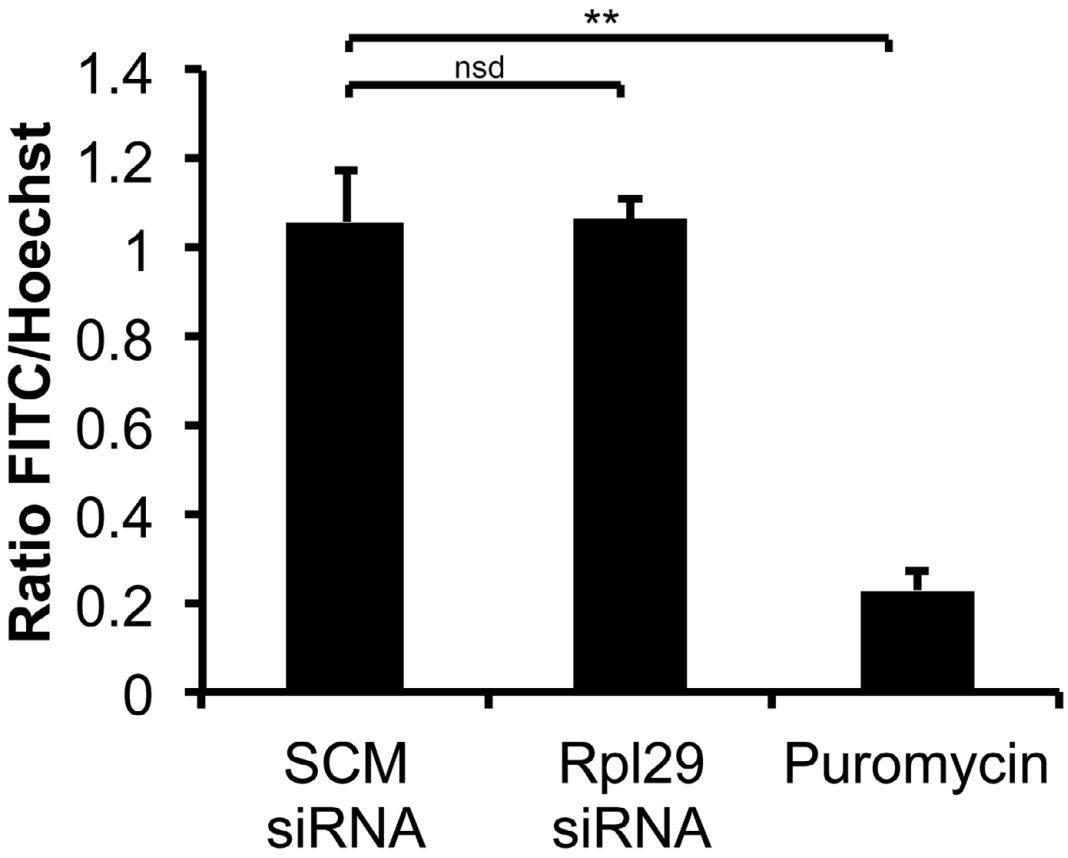

Fig. S11. Protein synthesis assay. Ten thousand cells were plated in each well of a 96-well plate pre-coated with PureCol (Nutacon), human plasma fibronectin (Millipore) and 0.1% gelatine. Protein synthesis was measured using Click-iT AHA Alexa Fluor 488 Protein Synthesis HCS Assay (Invitrogen) following the manufacturers protocol with methionine-free RPMI (Invitrogen). No significant difference was observed in protein synthesis between samples treated with *Rpl29* and SCM siRNA. Puromycin (1μM) was used as a positive control for protein synthesis inhibition. (n=3; nsd, not significant; **P<0.01).

Table S1. List of genes whose expression was upregulated in β*3*-null endothelial cells compared with wild-type (*P*<0.01).

Symbol	Accession	*P*-value	Definition
NeoR		4.4E-13	Neomycin resistant gene
Mcm6	NM_008567.1	4.7E-12	Minichromosome maintenance deficient 6
Rpl29	NM_009082.2	1.1E-11	Ribosomal protein L29
Fgfr1op2	NM_026218.1	4.9E-11	FGFR1 oncogene partner 2
Tm7sf1	XM_122498.1	2.5E-10	Transmembrane 7 superfamily member 1
Raet1c	NM_009018	1.2E-09	Retinoic acid early transcript gamma
Psmd8	NM_026545.1	2.1E-07	Proteasome (prosome macropain) 26S subunit non-ATPase 8
Cuedc1	NM_198013.1	2.2E-07	CUE domain-containing protein 1
Mgst1	NM_019946.3	3.7E-07	Microsomal glutathione *S*-transferase 1
Gdi3	NM_008112.2	6.2E-07	Guanosine diphosphate (GDP) dissociation inhibitor 3
9430077D24Rik	XM_135109	1.2E-06	RIKEN cDNA 9430077D24 gene
Rai3	NM_181444	1.3E-06	Retinoic acid induced 3
9630038C08Rik	AK036131	9.6E-05	
Cald1	AF439859.1	1.1E-04	h-caldesmon
9830123K24Rik	AK036507	1.4E-04	
Scarb2	NM_007644.2	3.0E-04	Scavenger receptor class B member 2
Cops8	NM_133805.2	3.8E-04	Constitutive photomorphogenic homolog subunit 8
5730409G07Rik	XM_126359.2	5.7E-04	RIKEN cDNA 5730409G07 gene
Atp2c1	NM_175025.2	6.8E-04	ATPase Ca^{++}-sequestering
Deadc1	NM_025748.2	8.7E-04	Deaminase domain containing 1
Ipo9	XM_129442.3	9.5E-04	Importin 9
Abhd1	NM_021304.2	1.3E-03	Abhydrolase domain containing 1
2010323F13Rik	NM_177157.2	1.9E-03	RIKEN cDNA 2010323F13 gene
2810417H13Rik	NM_026515.1	2.0E-03	RIKEN cDNA 2810417H13 gene
Thap4	NM_025920	2.3E-03	THAP domain containing 4
Pi16	NM_023734.2	2.5E-03	Peptidase inhibitor 16 precursor
Psmc4	XM_355872.1	2.5E-03	Prosome macropain 26S subunit ATPase 4
6430544H17Rik	NM_183140.1	2.6E-03	
Abhd1	NM_021304.2	2.7E-03	Abhydrolase domain containing 1
C430014G13Rik	AK049453	3.1E-03	Hypothetical protein
Tm7sf3	XM_132970.3	3.2E-03	Transmembrane 7 superfamily member 3
Acbd4	NM_025988.1	4.1E-03	Acyl-coenzyme A binding domain containing 4
Stk4	NM_021420.2	4.5E-03	Serine/threonine kinase 4
Insig2	NM_133748.1	5.5E-03	Insulin induced gene 2
Glis1	NM_147221.1	6.1E-03	GLIS family zinc finger 1
Mrpl3	AK054185	6.8E-03	Mitochondrial ribosomal protein L3
Nt5c3	NM_026004.1	6.8E-03	5-nucleotidase cytosolic III
Ugt1a9	NM_201410	7.0E-03	UDP glucuronosyltransferase 1 family, polypeptide A9
2610018I03Rik	XM_135023.2	7.1E-03	RIKEN cDNA 2610018I03 gene
B230312I18Rik	NM_172740.1	7.9E-03	RIKEN cDNA B230312I18 gene
Elmo1	NM_080288.1	8.5E-03	Engulfment and cell motility 1 ced-12 homolog
D730035F11Rik		9.1E-03	
Dgke	NM_019505	1.0E-02	Diacylglycerol kinase epsilon
E030030I06Rik	*XM_286230.2*	*9.9E-03*	*RIKEN cDNA E030030I06 gene*
Pnrc2	*NM_026383.1*	*8.2E-03*	*Proline-rich nuclear receptor coactivator 2*
Klra18	*NM_053153.1*	*8.1E-03*	*Killer cell lectin-like receptor subfamily A member 18*

Table S2. List of genes whose expression was downregulated in β3-null endothelial cells compared with wild-type (*P*<0.01).

Symbol	Accession	P-value	Definition
Rgs17	*NM_019958*	*7.6E-03*	*Regulator of G-protein signaling 17*
Agtrap	*NM_009642.3*	*7.6E-03*	*Angiotensin II type I receptor-associated protein*
Nr1d2	*NM_011584.2*	*6.7E-03*	*Nuclear receptor subfamily 1 group D member 2*
Mtap7	*NM_008635*	*6.4E-03*	*Microtubule-associated protein 7*
Klra22	*NM_053152.1*	*6.2E-03*	*Killer cell lectin-like receptor subfamily A member 22*
1810057P16Rik	*XM_126676.3*	*6.0E-03*	*RIKEN cDNA 1810057P16 gene*
E030030I06Rik	*XM_286230.2*	*5.3E-03*	*RIKEN cDNA E030030I06 gene*
1810041M07Rik	*AK007746*	*4.7E-03*	
D630046D15Rik	*AK052765*	*4.6E-03*	*Hypothetical BTB/POZ domain/Speract receptor (Scavenger receptor) containing protein*
Nt5	*AK047143*	*4.1E-03*	*5′ nucleotidase*
AI838661	*NM_133884.1*	*3.9E-03*	*Expressed sequence AI838661*
2610203C22Rik		*3.6E-03*	
Bcat1	*NM_007532.1*	*3.5E-03*	*Branched chain aminotransferase 1 cytosolic*
1810064L21Rik	*AK007954*	*2.9E-03*	
MGC67181	*NM_198619.1*	*2.8E-03*	*Unknown (protein for MGC:67181)*
3110001A05Rik	*AK013931*	*2.6E-03*	
2810408I11Rik		*2.5E-03*	
	AK021409.1	*2.4E-03*	*0 day neonate eyeball cDNA RIKEN full-length enriched library clone:E130302J09 product:hypothetical protein full insert sequence.*
LOC232532	*XM_132963.2*	*1.2E-03*	*Similar to IgE-binding protein*
Ehd3	*NM_020578.1*	*1.2E-03*	*EH-domain containing 3*
Hebp2	*NM_019487.2*	*1.1E-03*	*Heme binding protein 2*
2610305D13Rik	*NM_145078*	*1.0E-03*	*RIKEN cDNA 2610305D13 gene*
MGC67181	*NM_198619.1*	*9.3E-04*	
Raet1e	*NM_198193.1*	*9.2E-04*	*Retinoic acid early transcript 1E*
LOC381142	*XM_355058.1*	*7.3E-04*	*Similar to hypothetical protein FLJ38968*
C530044C16Rik		*2.4E-04*	
Cdkl2	*NM_177270.3*	*1.2E-04*	*Cyclin-dependent kinase-like 2 (CDC2-related kinase)*
Bcat1	*NM_007532.1*	*1.1E-04*	*Branched chain aminotransferase 1 cytosolic*
Fxr2h	*NM_011814*	*8.1E-05*	*Fragile X mental retardation gene 2 autosomal homolog*
Ybx3	*AK029441*	*8.0E-05*	*Y box protein 3*
Ppfibp1	*AK044496*	*7.9E-05*	*PTPRF interacting protein binding protein 1*
E030030I06Rik	*XM_286230.2*	*5.9E-05*	*RIKEN cDNA E030030I06 gene*
4933427D14Rik	*NM_028963.1*	*5.4E-05*	*RIKEN cDNA 4933427D14 gene*
1110005F07Rik	*NM_025383*	*1.7E-05*	*RIKEN cDNA 1110005F07 gene*
Abca5	*NM_147219.1*	*8.7E-06*	*ATP-binding cassette sub-family A (ABC1) member 5*
Hebp1	*NM_013546.1*	*8.2E-06*	*Heme binding protein 1*
Klra20	*NM_053150.1*	*4.8E-06*	*Killer cell lectin-like receptor subfamily A member 20*
Gp38	*NM_010329.1*	*1.8E-06*	*Glycoprotein 38*
LOC229810	*XM_124173.2*	*1.2E-06*	*Similar to Alpha enolase (2-phospho-D-glycerate hydro-lyase) (Non-neural enolase) (NNE) (Enolase 1)*
Itgb3	*NM_016780.1*	*6.9E-07*	*Integrin beta 3*
Raet1a	*NM_009016.1*	*4.2E-07*	*Retinoic acid early transcript 1 alpha*

Table S3. List of genes and primer sequences for real-time PCR.

Gene	Forward	Reverse
Actin	AAGGCCAACCGTGAAAAGAT	GTGGTACGACCAGAGGCATAC
β3-itgn	TCCAACATCTGTACCACACGA	GGGTGAGCCCTGAGACAA
Flk1	CAGTGGTACTGGCAGCTAGAAG	CAGTGGTACTGGCAGCTAGAAG
Rpl29	TCCGATGACATCCGTGACTA	CCATTTCTGTGCCATTTGC
Raet1γ	ATACACCAACGGGCTGGAT	CTTCGCTTCATACCAGAGAGG
Mgst1	ACTGACGAGAAGGTGGAACG	GAAGTGCATGAGGGCTGTAGA
Mcm6	ACCTGTACCACAATCTCTGCAC	CACCGCGTTTTACTTCATCA
Cuedc1	GGGACAAGTTGAAACACATGG	CTTCCTCATTTTGGTCTTCTCAG
Fgfr1op2	CCTTGAAGCACCTCAGCAC	TCTCGGTGATTTGGTCAACA
Gdl3	TGGAGGAGAAAGTGCGTCTATAA	CTGGCGGTTGTCCTGGTA
Psmd8	ATCCCTGCCGAAAGTTACAC	TAGGCCTTCTCAATGCATCC
Tm7sf1	AGTCAGAAATCCCACGAAGG	CGGGGGTTGTCAAAGAAGTA